

# A Novel Multi-Band Polarization Insensitive Frequency Selective Surface Based on Centrosymmetric L-Shaped Metal Strips

Yun Lin<sup>1</sup>, Xiaochun Xu<sup>1</sup>, Zheng Dou<sup>1</sup>, Xiaoxin Liu<sup>2</sup>, and Guohui Yang<sup>2</sup>

<sup>1</sup> College of Information and Communication Engineering  
Harbin Engineering University, Harbin, 150001, China  
douzheng@hrbeu.edu.cn

<sup>2</sup> School of Electronics and Information Engineering  
Harbin Institute of Technology, Harbin, 150001, China  
gh.yang@hit.edu.cn

**Abstract** — In this paper, a novel frequency selective surface (FSS) based on rotationally symmetric bended microstrips is investigated. The unit element consists of twelve L-shaped metal strips and a dielectric substrate. Bended L-shaped strips have different equivalent electric lengths corresponding to different resonant frequencies, which result in multi-band frequency characteristic. Meanwhile, the symmetric metal strips make the FSS polarization insensitive. The numerical experiments demonstrate that the FSS structure has fifteen stop-bands in the frequency band from 6 GHz to 20 GHz, and a good polarization stability as well. Moreover, the FSS design such as the inner radius of L-shaped metal strips, the dimensions of dielectric substrate and the width of the bended metal strips significantly effects on the FSS performance. Because of the multi-band property, the FSS designed in this paper has a bright prospect in many modern wireless communication systems and even in 5G communication system in the future.

**Index Terms** — Centrosymmetric bended micrstrip, FSS, multi-band, polarization insensitive.

## I. INTRODUCTION

Frequency selective surfaces (FSSs) are usually constructed by using a two-dimensional periodic metallic patterns combined with dielectric substrates [1, 2]. Generally, FSSs can be classified into two categories: (1) dipole array FSS, and (2)

slot array FSS, and the former exhibits band-stop characteristic while the later exhibits band-pass characteristic. FSSs have been widely used as spatial filters to totally reflect or just transmit electromagnetic waves in some specified frequency bands [3]. FSSs can be applied in antenna radome, filter, radar cross section (RCS) reduction, directivity enhancement and dichroic sub-reflector. Theoretically, FSS is an infinite array with a periodic structure; however, it is always finite in practical applications. The truncation of the infinite period structure will change the FSS performance, which makes it necessary to utilize sufficient elements to keep the characteristics of infinite FSS [4].

One of the important FSS applications is to work as sub-reflectors for the satellite communication so that a single main reflector can cover the different frequency bands [5, 6]. To enhance the capability of multi-frequency and multi-function antennas, a sub-reflector integrated with FSS is operated normally at multi-band frequencies; meanwhile, FSS is polarization insensitive in multi-bands [7]. In addition, the increasing demands on multi-functionality of antennas for communications also require multi-band polarization insensitive FSSs. To design multi-band insensitive polarization FSS, some ideas such as gradient variation structure and fractal shape are proposed [8, 9]. However, the transmission of gradient variation structure FSS is usually not low enough in stop-bands, while the number of stop-bands of a fractal shape FSS is

tightly restricted within three. Moreover, most existing multi-band FSSs are sensitive to polarization.

The modern wireless communication system is developing to multi-standard and multi-system, which requires the radio frequency filter in the system to have multi-band function in many cases. In this paper, a novel multi-band polarization insensitive FSS is designed, which has the top layer composed of twelve centrosymmetric bended metal strips. Because rotationally symmetric bended metal strips can resonate at different frequencies, the FSS had fifteen stop-bands in the frequency band from 6 GHz to 20 GHz for both TE and TM wave. In addition, FSS is only 2 mm in thickness, which grants the FSS broad application prospects in fabricating sub-reflector due to its light weight and low cost. And owing to its multi-band property, the FSS designed in this paper could be used in modern wireless communication system and even 5G communication system in the future. Moreover, the pass-bands and stop bands can be easily changed by changing the geometry size of the FSS, which makes the FSS more promising in application.

## II. FSS STRUCTURE AND ANALYSIS

### A. Basic multi-band polarization insensitive FSS design

A multi-band polarization insensitive FSS with a simple configuration is designed in this section whose unit cell is shown in Fig. 1. The top layer of the FSS is composed by four bended metal strips whose length is  $a = 10.0$  mm, width is  $w = 1.0$  mm and thickness is 0.035 mm. Two of the metal strips are put in horizontal, while the other two are put in vertical to ensure the FSS polarization insensitive. The spacing between two metal strips is  $d = 8.0$  mm. The length of the dielectric substrate is  $A = 30.0$  mm and its thickness is  $D = 2.0$  mm. The relative permittivity of substrate slab is  $\epsilon_r = 2.2$ .

In order to simulate the infinite periodic array of FSS accurately, periodic boundary conditions (PBC) are utilized to top, bottom, left and right boundaries, while open (add space) boundary conditions are utilized to front and back boundaries of the unit cell in electromagnetic (EM) simulation software CST MICROWAVE STUDIO 2012. Frequency domain solver and tetrahedral mesh are used to make the simulation. And for the purpose of getting accurate simulation results, high initial

mesh density and adaptive tetrahedral mesh refinement are utilized during the simulation. The transmission of the FSS for TE and TM incident waves is plotted in Fig. 1. The frequency band with transmission of higher than -3 dB is called as a pass-band while that with transmission of lower than -10 dB is defined as a stop-band. It can be seen from Fig. 1, that the FSS has six stop-bands and seven pass-bands in the frequency band from 6 GHz to 20 GHz and has the same responses for TE and TM wave. However, the number of pass-bands is not great enough and some frequency spaces of adjacent pass-bands are too narrow.

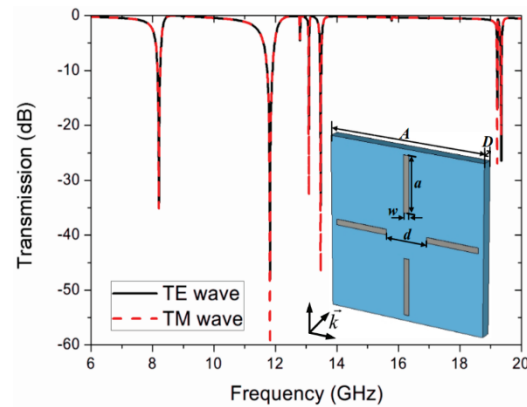


Fig. 1. Transmission coefficients and configuration of the basic FSS unit cell.

### B. Improved multi-band polarization insensitive FSS design

In purpose of increasing the pass-bands number and reasonably arranging the frequency spaces of adjacent pass-bands. An improved multi-band polarization insensitive FSS based on centrosymmetric fold lines is proposed in this section, whose configuration is illustrated in Fig. 2. In detail, centrosymmetric L-shaped metal strips are used in the FSS unit cell. According to the electromagnetic wave theory, the resonant frequency of the metal unit cell is relevant to its size, which means the FSS could resonate in case that the total effective length of the unit cell is roughly equal to the wavelength  $\lambda$  of the incident electromagnetic wave. It can be seen from Fig. 2, that the unit cell structure has 6 different effective lengths for incident EM waves (TE wave and TM wave), which makes the FSS have 6 different basic resonant frequencies and 6 corresponding basic stop-bands. Besides, some high-order resonances

could also be excited which could further increase the number of stop-bands of the FSS. That is the reason why L-shaped metal strips are selected in the paper.

For the purpose of comparison with the FSS designed in Section II. A, the dimension parameters of the unit cell are given as follow. The thickness of the bended metal strips is 0.035 mm. The lengths of two arms of L-shape are  $a_1 = 10.0$  mm and  $a_2 = 6.0$  mm, and the width of L-shaped metal strips is  $w = 1.0$  mm, as shown in Fig. 1. The inner radius of "L" pattern is  $r = 4.0$  mm, and the rotation angle between two adjacent L-shaped metal strips is  $\alpha = 30^\circ$ . The length, thickness and relative permittivity of the dielectric substrate are the same as the FSS designed in Section 2.1.

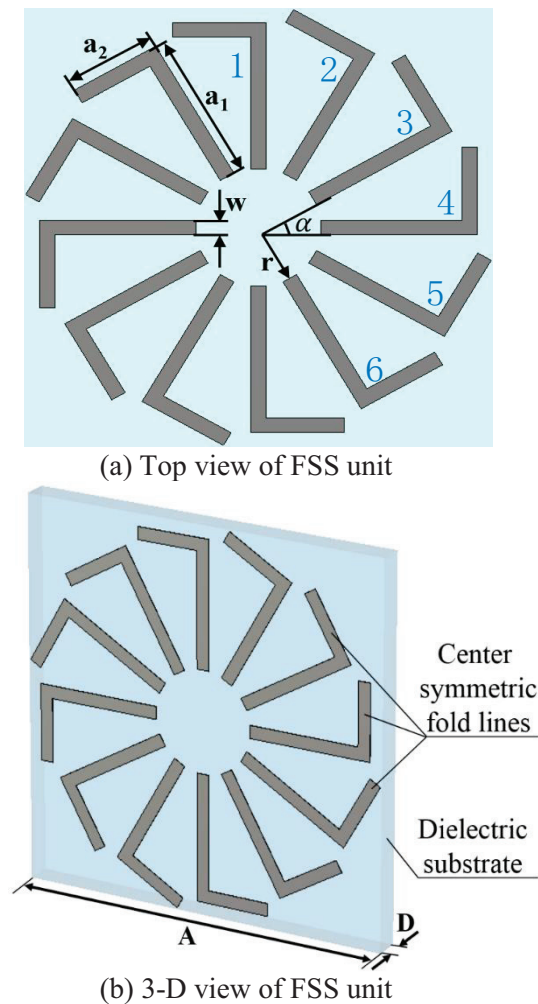


Fig. 2. Configuration of the improved FSS unit cell.

The unit cell is truncated by using PBC in CST

MWS 2012 and the simulation settings including boundary conditions and mesh type are same as Section II. A. Figure 3 shows the transmission of the FSS structure for the TE and TM incident waves. It can be seen from Fig. 3, that the FSS structure has fifteen stop-bands and sixteen pass-bands in the frequency band from 6 GHz to 20 GHz, and the frequency ranges of the sixteen pass-bands are illustrated in Table 1. In addition, it can be observed that transmission of the FSS for TE and TM waves is nearly identical, which verifies that the FSS is polarization insensitive.

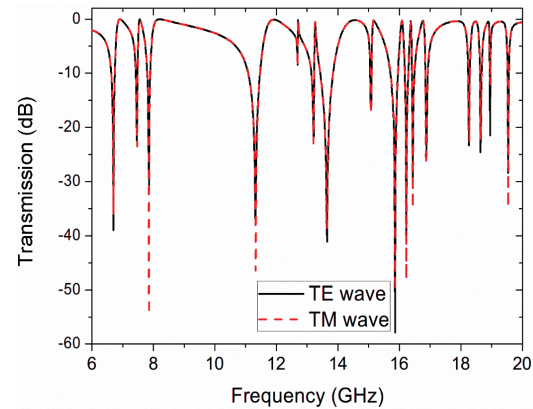


Fig. 3. Transmission coefficients of the improved FSS structure for TE and TM waves.

Table 1: Frequency ranges of sixteen pass-bands

Pass-band Number	1st	2nd	3rd	4th
Frequency Range (GHz)	6.00-6.30	6.78-7.30	7.50-7.70	7.95-10.18
Pass-band Number	5th	6th	7th	8th
Frequency Range (GHz)	11.62-12.76	13.23-13.30	14.10-14.98	15.10-15.42
Pass-band Number	9th	10th	11th	12th
Frequency Range (GHz)	16.02-16.14	16.34-16.40	16.63-16.82	17.10-18.18
Pass-band Number	13th	14th	15th	16th
Frequency Range (GHz)	18.34-18.58	18.74-18.92	18.98-19.47	19.61-20.00

Comparing with the simulation results of the FSS proposed in Section II. A, it can be observed that the improved FSS has 16 stop-bands which is over three times as much as the former one. Meanwhile, the pass-bands of the improved FSS are distributed more evenly in frequency which makes the FSS more valuable in real application. In addition, it can be seen from Fig. 1 to Fig. 3, that in same conditions the stop-bands move to lower frequencies which results from the longer effective lengths of improved unit cell.

In order to explore the multi-band frequency property of the proposed FSS, eight valley points in the transmission pattern are selected as examples. The surface current distributions at the eight frequencies for TE wave are illustrated in Fig. 4. It can be seen from the figure that different L-shaped metal strips resonate at different frequencies. For example, at 6.70 GHz, the two L-shaped metal strips in the vertical direction resonate; while at 7.46 GHz, the two L-shaped metal strips at an angle of 30 degrees to the horizontal direction resonate. The reason why different metal strips resonate at different frequencies is that the length at different angles for TE wave is different, which can be expressed as follows:

$$\begin{aligned} l_e &= a_1 \cos(90^\circ - \alpha) + a_2 \sin(90^\circ - \alpha) \\ &= a_1 \sin \alpha + a_2 \cos \alpha, \end{aligned} \quad (1)$$

where  $\alpha$  is the angle between one L-shaped metal strips with respect to the horizontal axis, and  $l_e$  is the equivalent length of L-shaped metal strips. Obviously, the resonant frequencies of L-shaped metal strips increase with decrease of equivalent length  $l_e$ , which results in the multi-band frequency property. Moreover, the FSS structure has some additional resonant modes besides single L-shaped metal strips resonant modes such as Figs. 4 (g) and 4 (h), which make the FSS have more stop-bands.

To explain the simulation results in detail, physical interpretations are given below.

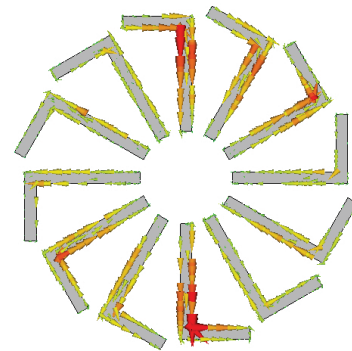
The reflectivity  $S_{11}$  of the FSS can be described by (2):

$$|S_{11}| = \left| \frac{Z_{in} - Z_0}{Z_{in} + Z_0} \right|, \quad (2)$$

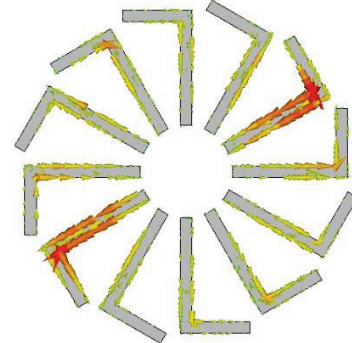
where  $Z_{in}$  is the input impedance of FSS and  $Z_0$  is the wave impedance of free space. It can be learned from (2), that  $Z_{in} = Z_0$  is necessary to decrease the reflective wave and in that case  $S_{21}$  of the FSS is possible to be kept in a high value.

In the condition that L-shaped strips do not

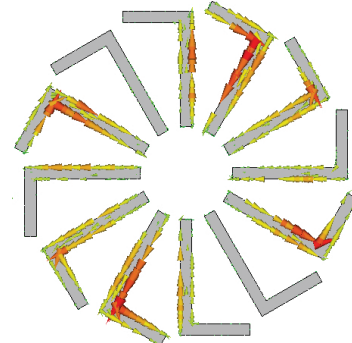
resonate, the incident EM waves can propagate through the FSS easily because the input impedance  $Z_{in}$  is close to the free space wave impedance  $Z_0$ , and the reflectivity  $S_{11}$  is quite small. Then in the condition that L-shaped strips resonate, the input impedance  $Z_{in}$  has a sharp change around the resonance frequency which makes the value of  $Z_{in}$  not close to  $Z_0$  anymore and results in a high reflectivity  $S_{11}$ , which means the incident wave cannot propagate through the FSS. In general, the FSS will have a stop-band in case that the unit cell resonates at a frequency. Because of the multi-resonance property of the unit cell, the FSS proposed in the paper has such many pass-bands and stop-bands in the frequency band from 6 GHz to 20 GHz.



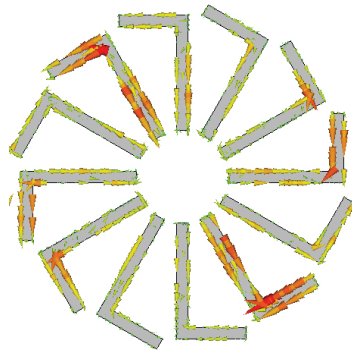
(a) The case at 6.70 GHz



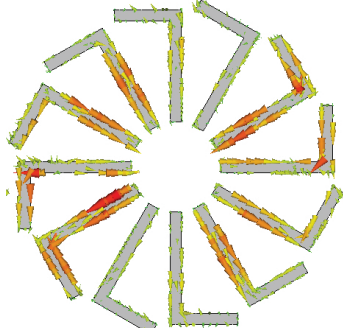
(b) The case at 7.46 GHz



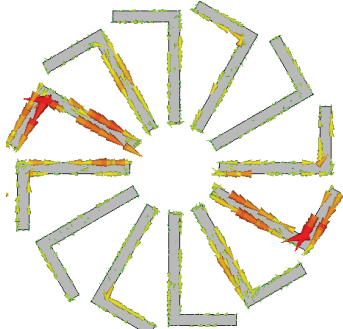
(c) The case at 7.86 GHz



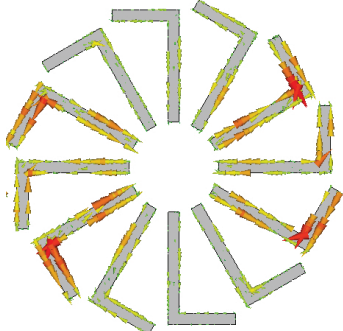
(d) The case at 15.86 GHz



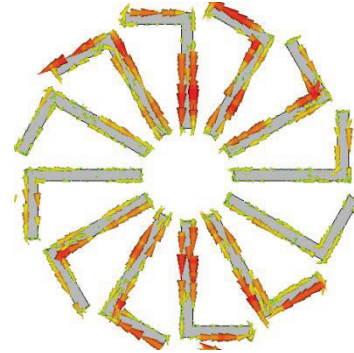
(e) The case at 16.22 GHz



(f) The case at 16.88 GHz



(g) The case at 16.43 GHz



(h) The case at 18.84 GHz

Fig. 4. Surface current distributions at the eight typical frequencies for TE incident wave.

The simulation results of the surface current distributions for TM incident wave are almost the same as those for TE wave. These simulation results verify the polarization insensitive property of the proposed FSS structure.

### III. EFFECTS OF THE STRUCTURE PARAMETERS ON THE FSS

#### A. The distance between symmetric center and one end of fold line $r$

To explore the FSS amplitude-frequency characteristic, we change the inner radius  $r$  from 2.0 mm, 3.0 mm to 4.0 mm. The transmission coefficient in the frequency band of 10-15 GHz for TE wave is illustrated in Fig. 5. It can be seen from Fig. 5, that the trend of resonant frequency varies with different valley points when  $r$  increases. When the frequency at the first valley point increases, the frequencies at the second and the third valley points remain invariant, while the frequency at the last valley point decreases. It is the reason why the FSS structure has some additional resonant modes besides single L-shaped metal strips resonant modes. For these complex resonant modes, the effect analyses of  $r$  on the FSS property are difficult, while for a single L-shaped metal strips resonant mode, the inner radius has little effect on the resonant frequencies.

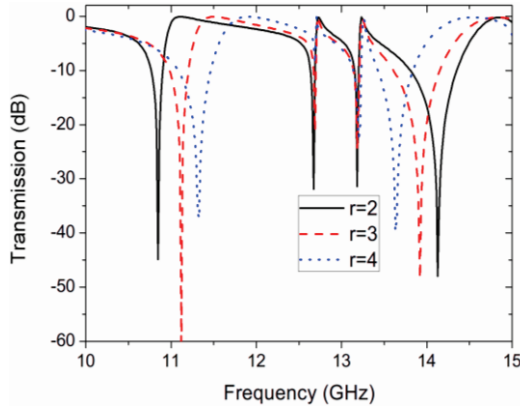


Fig. 5. Transmission coefficients of the FSS structure with different inner radius  $r$ .

**B. The side length of dielectric substrate  $A$**

Change the length and width of dielectric substrate  $A$  to be different values from 30.0 mm to 32.0 mm, 34.0 mm to 36.0 mm, and the transmission coefficients of the FSS structure in the frequency band of 9 to 14 GHz for TE wave are plotted in Fig. 6. The resonant frequencies decrease with the increase of  $A$  and the deepness of valley points varies at the same time, which is mainly caused by the coupling of adjacent unit cells. Generally speaking, smaller  $A$  is necessary for its good effects on suppressing grating lobe and widening the band width.

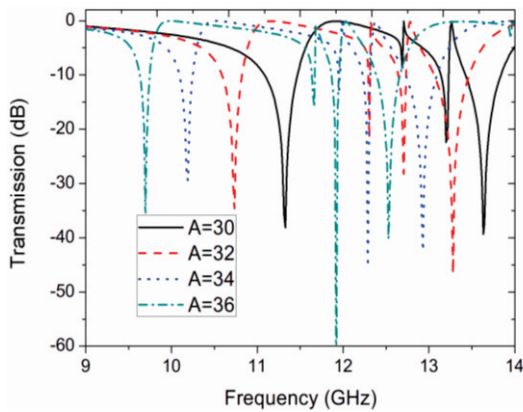


Fig. 6. The transmission of the FSS with different side lengths of dielectric substrate  $A$ .

**C. Width of fold lines  $w$**

In this section, we change the width of L-shaped metal strips  $w$  to be different values from 0.4 mm, 1.0 mm to 1.6 mm to investigate the FSS

amplitude-frequency characteristic. Figure 6 shows the transmission coefficients of the FSS structure in the frequency band of 10 to 15 GHz for TE wave. It can be seen from Fig. 7, that the trend of resonant frequency is ruleless with the increase of  $w$  due to the multi-resonant modes of the FSS structure. In other words, the width of L-shaped metal strips  $w$  has different effects on the transmission property under different resonant modes. However, it can be summarized that increasing  $w$  is beneficial for deepening the deepness of valley points at resonant frequencies.

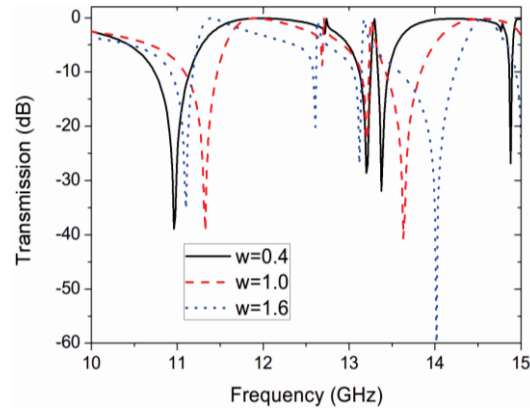


Fig. 7. The transmission of the FSS with different widths of fold lines  $w$ .

**IV. CONCLUSIONS**

In summary, a novel multi-band polarization insensitive FSS based on rotationally symmetric L-shaped metal strips is proposed in this paper. The FSS structure is polarization insensitive due to the symmetric structure; meanwhile, different L-shaped metal strips had different equivalent lengths for electromagnetic wave to resonate at different frequencies that grant the FSS structure an excellent multi-band property. According to simulation results, the FSS structure had fifteen stop-bands and sixteen pass-bands for TE and TM waves in the frequency band of 6 to 20 GHz. In addition, effects of some structure parameters are analyzed, which can provide theoretical basis for practical use. Owing to the great multi-band property and thin, light and flexible features, the FSS designed in this paper is believed to have broad application prospects in modern wireless communication system and even 5G communication system in the future.

## ACKNOWLEDGMENT

This work is supported by the Nation Nature Science Foundation of China No. 61301095 and 61201237, and Nature Science Foundation of Heilongjiang Province of China No. QC2012C069.

Meantime, all the authors declare that there is no conflict of interests regarding the publication of this article.

## REFERENCES

- [1] T.-K. Wu, *Frequency Selective Surfaces*, Encyclopedia of RF and Microwave Engineering: John Wiley & Sons, Inc., 2005.
- [2] S. A. Winkler, W. Hong, M. Bozzi, and K. Wu, "Polarization rotating frequency selective surface based on substrate integrated waveguide technology," *Antennas and Propagation, IEEE Transactions on*, vol. 58, no. 4, pp. 1202-1213, 2010.
- [3] B. A. Munk, *General Overview, Frequency Selective Surfaces*, John Wiley & Sons, Inc., pp. 1-25, 2005.
- [4] H. Y. Yang, S. X. Gong, P. F. Zhang, F. T. Zha, and J. Ling, "A novel miniaturized frequency selective surface with excellent center frequency stability," *Microwave and Optical Technology Letters*, vol. 51, no. 10, pp. 2513-2516, 2009.
- [5] S. Monni, A. Neto, G. Gerini, F. Nennie, and A. Tijhuis, "Frequency-selective surface to prevent interference between radar and SATCOM antennas," *Antennas and Wireless Propagation Letters, IEEE*, vol. 8, pp. 220-223, 2009.
- [6] J. P. Gianvittorio, J. Romeu, S. Blanch, and Y. Rahmat-Samii, "Self-similar prefractal frequency selective surfaces for multiband and dual-polarized applications," *Antennas and Propagation, IEEE Transactions on*, vol. 51, no. 11, pp. 3088-3096, 2003.
- [7] K. Ueno, T. Itanami, H. Kumazawa, and I. Ohtomo, "Characteristics of frequency selective surfaces for a multi-band communication satellite," *IEEE AP-S Int. Symp. Dig.*, pp. 735-738, June 1991.
- [8] J. Romeu and Y. Rahmat-Samii, "Fractal FSS: a novel dual-band frequency selective surface," *Antennas and Propagation, IEEE Transactions on*, vol. 48, no. 7, pp. 1097-1105, 2000.
- [9] D. J. Kern, D. H. Werner, A. Monorchio, L. Lanuzza, and M. J. Wilhelm, "The design

synthesis of multiband artificial magnetic conductors using high impedance frequency selective surfaces," *Antennas and Propagation, IEEE Transactions on*, vol. 53, no. 1, pp. 8-17, 2005.



**Yun Lin** (S'99-M'03) received his Ph.D. degree in Communication and Information in 2010 from Harbin Engineering University, Harbin, China. He joined the Information and Communication College, HEU, Harbin, China, in 2005, where he is currently a Professor, Vice-Dean of ICEC College, Director of the Smart Communications Lab for ICEC. His research has focused on information fusion, signal processing and EMC on antenna, mm-wave and THz. He has authored and co-authored over 5 papers in refereed journals and conference proceedings.



**Xu Xiao-chun** stayed in Harbin Engineering University (HEU) to read her B.E. during 2009-2013, and received her B.E. in the College of Underwater Acoustic Engineering from HEU in 2013. She reads her M.A. in Harbin Engineering University and is studying Signal Processing.



**Zheng Dou** (S'97-M'01) received his Ph.D. degree in Communication and Information in 2007 from Harbin Engineering University, Harbin, China. He joined the Information and Communication College, HEU, Harbin, China, in 2001, where he is currently a Professor, Vice-Dean of ICEC College, Director of the Smart Communications Lab for ICEC. He spent one year as a Research Fellow and an Invited Professor at the University of Hertford, Hatfield, UK, and three months as a Visiting Professor at Wright University, USA in 2013. His research has focused on Smart Communications and EMC, which includes all-one platform on Smart

Communications, Architecture and protocols, EMC on antenna, mm-wave and THz, IR-UWB communications and signal processing. Dou has

authored and co-authored over 2 papers in refereed journals and over 30 papers in conference proceedings.